Hindawi
Wireless Communications and Mobile Computing
Volume 2022, Article ID 5995213, 8 pages
https://doi.org/10.1155/2022/5995213

Research Article

Modeling and Performance Optimization of a Compact Three-Petalled Flower-Like Microstrip Patch Antenna for IoT Applications

Nancy Gupta,[1] **Navneet Gill**,[1] **and Fidele Maniraguha**[2]

[1]*Department of Electronics & Communication Engineering, School of Engineering, Lyallpur Khalsa College Technical Campus, Jalandhar, Punjab, India*
[2]*University of Rwanda, College of Science and Technology, African Center of Excellence in IoT, Rwanda*

Correspondence should be addressed to Fidele Maniraguha; manifils@gmail.com

Received 5 April 2022; Revised 25 May 2022; Accepted 28 May 2022; Published 17 June 2022

Academic Editor: Kuruva Lakshmanna

The article is aimed at proposing the design and investigating the performance of a three-petalled flower-shaped wideband microstrip patch antenna for IoT and next-generation wireless applications. The proposed printed monopole antenna is provided with a microstrip feed line for excitation with a defected ground plane. The antenna is designed and analyzed using a finite-element-based simulator HFSS (version 15.0). The Optimetrics feature in the simulator is used for the performance optimization of the designed antenna that results in wide impedance bandwidth between 2.5 and 5.5 GHz, with add-on benefits such as less human efforts along with fast optimum results. The designed antenna holds an advantage of being low profile and reduced in size as overall diminutive dimensions of the proposed patch antenna are $0.54\,\lambda_o \times 0.43\,\lambda_o \times 0.021\,\lambda_o\,\text{mm}^3$, making it suitable for use in Wi-Max- and WLAN-enabled IoT applications. The paper is aimed at proposing an innovative optimal design aiming at the concerns about the risks in the growth of IoT and mobile computing, particularly in wireless and mobile networks. The anticipated antenna, owing to its simple and compact design, can be easily integrated into portable mobile devices, and thus, it is considered suitable for 4G and 5G and other next-generation communication applications of IoT devices.

1. Introduction

With the advent of the modern technology, antennas have become the most essential component of wireless communication systems as they characterize the main medium of transmission and reception of signals. Vitally, an antenna represents the system accountable for the conversion of the guided waves of the transmission line into space, over short distances ranging from a few centimeters to long distances of hundreds of kilometers [1, 2]. All modern wireless systems require efficient and economical antennas that possess features such as light weight and wide impedance bandwidth. It is also desirable to develop such antennas that work at multiple frequency bands peculiar to number of next-generation wireless applications [3]. Microstrip patch antennas are one among the favourable contenders that ensure inherent advantages such as small dimensions, light weight, less fabrication expenditure, and planar structure [4, 5].

Internet of things (IoT) can be visualized as an integrated network where infinitude of IoT sensors, computers, mobile phones, and other IoT devices could be connected through Internet so as to communicate information within its environment and at remote distances [6, 7]. This technology has seen tremendous growth in the latest era of wireless communications particularly in fields of education, home automation, health sectors, industry, and many other relevant applications [8–15]. Therefore, the amalgamation of massive IoT devices into the daily life use has raised the need for developing new algorithms and techniques to cope with the different challenges from the connected devices [16]. The number of allied devices via IoT is expected to upsurge to 30 billion by 2025, and performing actions such as

environment sensing, collecting data, and transferring it to a data handling station is energy-consuming [17]. Low-Power Wide-Area Network (LPWAN) has established itself as the preferred option for IoT networks due to its long communication range, low energy consumption, and low cost. LPWAN protocols can provide connectivity for many low-power battery-operated devices for delay-tolerant applications with limited throughput per device [18]. Microstrip patch antennas are generally preferred in IoT applications due to their compatibility and ease of integration inside the IoT devices. Thus, various researchers are working towards designing of broadband/wideband microstrip antennas for IoT-based applications using number of techniques such as innovative patch antennas' shapes and designs, using a varied range of available antenna feeding methods, presenting different slot structures, shorting pins, stacking of patch antennas, metamaterials, defected/partial ground planes, electromagnetic bandgap materials, etc. [19].

Chattha et al. [20] designed compact W-shaped printed multiband frequency reconfigurable (over 8 bands) patch antenna for 4G LTE applications. Gupta et al. [19] proposed a wideband diagonally symmetrical flower-shaped patch antenna with reduced ground plane that provides wide impedance bandwidth between 1.49 and 2.46 GHz. It is suitable for GPS (1.57 GHz), GSM (1.8 GHz), Wi-Max (2.3 GHz), and WLAN (2.45 GHz) portable applications. Additionally, the authors [5] investigated the performance of planar and compact CPW-fed microstrip patch antenna in another research work that offers 10 dB impedance bandwidth over the wide frequency range between 2.59 and 7.61 GHz over various parametric design variables. This compact antenna offers a 10 dB wide impedance bandwidth of 5.02 GHz. Tripathi et al. [21] proposed compact and slotted patch antenna geometry of size (30.8×37.2 mm) and investigated it at frequency 3.30 GHz. The projected antenna covers 2.08–3.99 GHz frequency band suitable for S-band (2–4 GHz) wireless communication.

Khan et al. [22] proposed a miniaturized microstrip antenna with stable transmission characteristics and omnidirectional coverage so that it can be easily integrated in IoT-enabled smart devices. Similarly, Varum et al. [23] introduced a compact wideband microstrip antenna array so as to accomplish wide impedance bandwidth for use in IoT/5G systems. The substrate used was Rogers RO4350B along with conventional ground plane on opposite side to result in a high-gain antenna for the desired applications. Rani and Singh [24] present a novel design of a printed hybrid fractal tree (PHFT) antenna using bacterial forging optimization (BFO) in aggregation with a curve fitting technique. The antenna design is created on the hybrid structure obtained by combining meander line geometry with fractal tree, whose geometrical descriptors are determined by means of BFO.

Abdulkawi et al. [25] proposed novel low-cost single- and dual-band microstrip patch antennas on a square microstrip patch etched symmetrically with four slots. The antenna is constructed to have low cost and reduced size to be used in Internet of things (IoT) applications. The antennas provide a reconfigurable architecture that allows operation in different wireless communication bands. Ramasamy et al. [26] proposed a bloom-shaped antenna which runs at multiband frequencies between 1.6 GHz and 2.45 GHz using FR4 substrate material being easily available at low cost. The proposed antenna structure has been simulated and analyzed in different experimental results including return loss measurement, voltage standing wave ratio measurement, radiation pattern measurement, and gain measurement. Islam et al. [27] have proposed modified meander shape microstrip patch antenna for IoT applications at 2.4 GHz ISM band. The antenna design is comprised of an inverse S-shape meander line coupled with a slotted rectangular box to which a capacitive load (C-load) and parasitic patch with the shaped ground are applied.

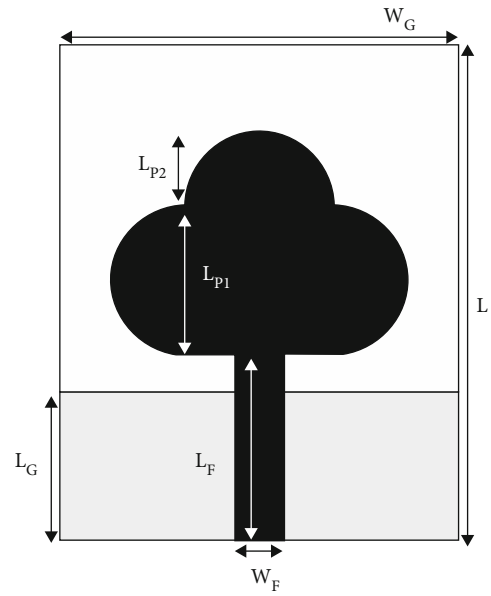

Figure 1: Proposed antenna design structure.

However, the conventional design of the antenna using any electromagnetic simulator requires repetitive simulations based on a trial and error method that wastes hours of human efforts. Various optimization and machine learning algorithms have been proven to provide solution to this conventional approach of iterative hit-and-trail-based simulations [28, 29]. In this proposed research work, a compact antenna with the diminutive dimensions of $40 \times 32 \times 1.6\,\text{mm}^3$ is designed and optimized using Optimetrics feature available in the electromagnetic simulator termed as high-frequency structure simulator (HFSS) (version 15.0). With the assistance of constrained super linearly convergent optimization tool integrated in the simulator, the optimum 10 dB wide impedance bandwidth is attained between 2.5 and 5.5 GHz with less time and reduced efforts. Additionally, due to the compact and miniaturised size of the proposed antenna, it is found to be highly suitable for the IoT applications. The advantage of this antenna size diminishment is that it allows easy incorporation into the regularly small and compact IoT devices.

The rest of article is framed as follows: the proposed design and its specifications are included in Section 2. The discussion on parametric variation of different design variables using the Optimetrics tool in HFSS is given in Section

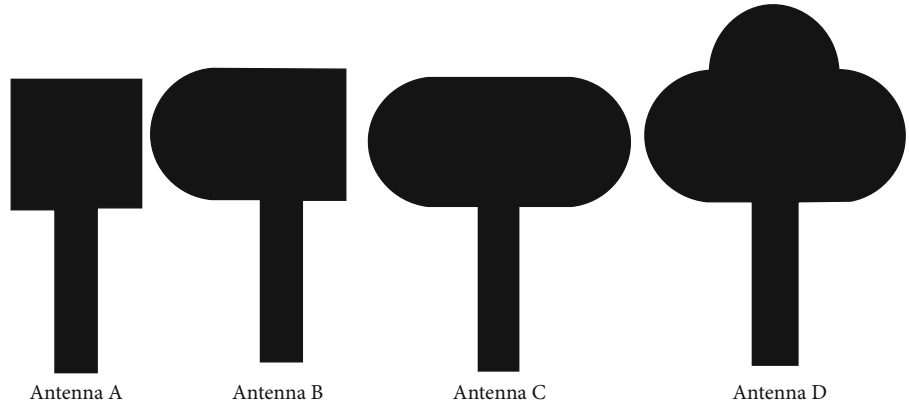

Figure 2: Evolution of the final patch radiator.

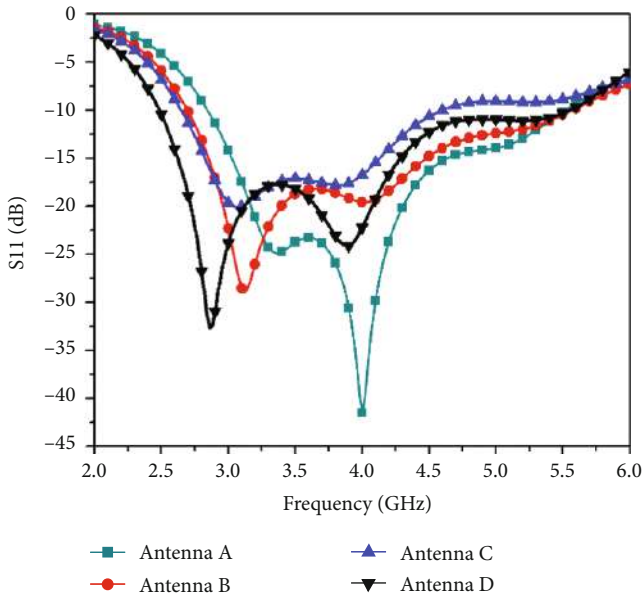

Figure 3: Simulated S_{11} parameter for various antenna designs.

Table 1: Dimensions for the proposed antenna structure.

Parameters	L	W_G	L_G	L_{P1}	L_F	W_F
Units (mm)	40	32	12	12	15	4

3. The results and their discussions comprise Section 4 with brief conclusion presented in Section 5.

2. Proposed Antenna Design Considerations

The introduced antenna is created using a square patch of side length L_{P1}. Three semicircles are appended at three sides of square patch with the radius (L_{P2}) of each semicircle as half of square's side length, L_{P1}, i.e., the radius; L_{P2} of semicircles shares the following relation with the square patch:

$$L_{P2} = \frac{L_{P1}}{2}. \quad (1)$$

A microstrip line feed with dimensions ($L_F \times W_F$) is provided at the bottom end of the designed square patch which is connected with 50 Ω SMA (subminiature version-A) connector at the opposite end. The length and width of the microstrip feed are optimized through the parametric analysis in order to acquire the wide bandwidth suitable for WLAN/WiMAX portable applications. The antenna structure is constructed using FR4-epoxy substrate which has dielectric constant of 4.4 with dielectric loss tangent of 0.02. The chosen substrate possesses the benefit of being mechanically robust and cost-effective along with easily available access in the market. The partial ground plane with dimensions ($L_G \times W_G$) is added at the opposite side of the chosen substrate that adds to the 10 dB impedance matching over the desired frequency band. The length L_G is selected after optimization using parametric analysis through the electromagnetic simulator. The anticipated antenna is compact in size with overall dimensions of $0.54\,\lambda_o \times 0.43\,\lambda_o \times 0.021\,\lambda_o\ \text{mm}^3$ (shown in Figure 1).

Figure 2 illustrates how the final patch antenna design is created so as to achieve the wide-impedance bandwidth between 2.5 and 5.5 GHz frequency range. Initially, the square patch antenna with side length L_{P1} and microstrip feed line ($L_F \times W_F$) is analyzed that resulted in 10 dB impedance bandwidth between 2.86 and 5.52 GHz. With the aim of shifting the resonance response to cover the 2.5 GHz band specifically for WLAN-enabled IoT applications, one semicircle with radius as half of side length of initial square patch design is introduced on the left side. With the introduced modification, the 10 dB bandwidth shifted down to 2.7–5.56 GHz. For further reducing the resonance to lower side, another semicircle with similar dimensions is attached at the opposite side of the square patch, which provided 10 dB impedance bandwidth between 2.66 and 4.58 GHz. Although the 10 dB impedance frequency response shifted to the lower side, there is slight reduction observed in the bandwidth. Thus, by seeking additional improvement in bandwidth response, another semicircle, with same dimensions as other two, is appended at the top side of the square patch. The final patch design has acquired the optimal wide-impedance bandwidth between 2.5 and 5.5 GHz. The S_{11}

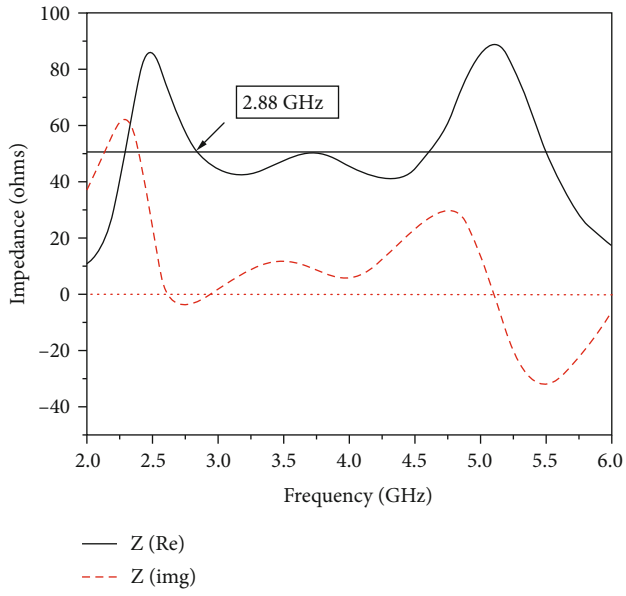

Figure 4: Input impedance for the proposed antenna design.

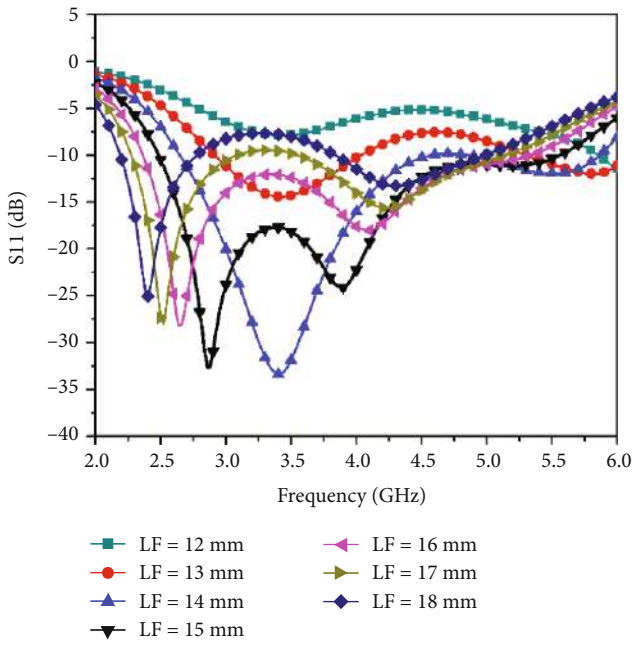

Figure 5: Effect of feed length on S_{11} response against frequency.

parameters simulated for each antenna design in order to analyze the improvement in terms of impedance bandwidth are shown in Figure 3.

As the antenna is printed monopole type structure, its lower resonant frequency can be estimated as follows [30, 31]:

$$f_r = \frac{14.4}{l_1 + l_2 + g_1 + \left(A_1/2\pi l_1\sqrt{(\varepsilon_r+1)/2}\right) + \left(A_2/2\pi l_2\sqrt{(\varepsilon_r+1)/2}\right)}\ \text{GHz}, \tag{2}$$

where l_1 and l_2 denote the length of the ground plane and

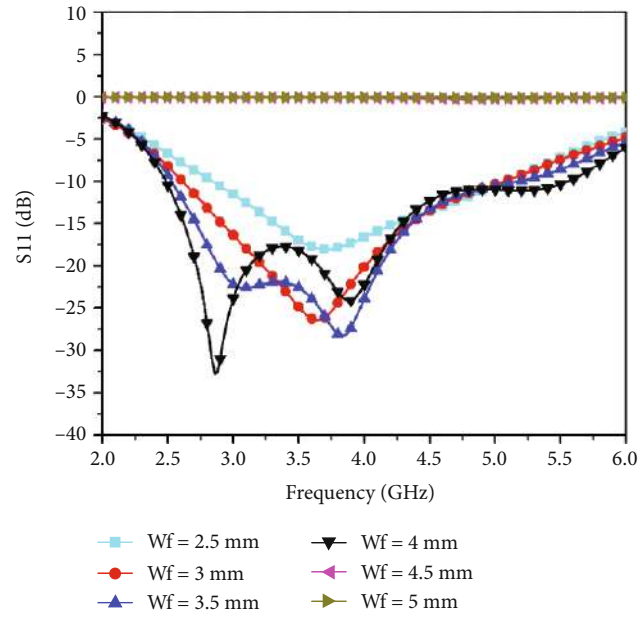

Figure 6: Effect of feed width W_F on S_{11} response against frequency.

conducting patch, respectively. g_1 represents the gap between radiating patch and partial ground plane. A_1 and A_2 indicate the calculated area for the ground plane and patch radiator, respectively. All l_1, l_2, g_1, A_1, and A_2 are considered in centimeters. ε_r is the dielectric constant of the substrate.

For the proposed antenna design, the parameters required as per equation (2) are calculated as follows:

Length of ground plane: $l_1 = L_G$.

Length of the conducting patch:

$$l_2 = L_F + L_{P1} + L_{P2}. \tag{3}$$

Gap between the patch radiator and ground plane:

$$g_1 = L_F - L_G. \tag{4}$$

Area of the ground plane: $A_1 = (L_G \times W_G)$.

Area of the radiating patch:

$$A_2 = 3\left[\frac{\pi L_{P2}^2}{2}\right] + \left[L_{P1}^2\right] + \left[L_F \times W_F\right]. \tag{5}$$

As per data available from Table 1, the lower resonant frequency is calculated to be $2.758 \approx 2.8$ GHz. When the proposed antenna structure is simulated through the 3D electromagnetic solver, the lower simulated resonant frequency is attained at 2.88 GHz which is in close agreement with the calculated frequency using equation (2). The impedance matching obtained at 2.88 GHz can be verified from the simulated graph of input impedance as shown in Figure 4.

Input impedance is complex impedance offered by the antenna at its input terminals. If there is proper impedance matching between the characteristic impedance of

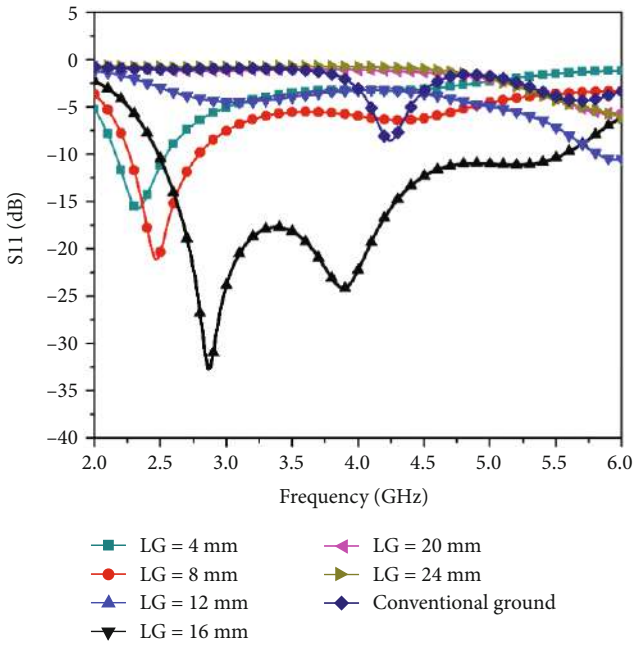

Figure 7: Effect of variation in length of the partial ground plane L_G on S_{11} response against frequency.

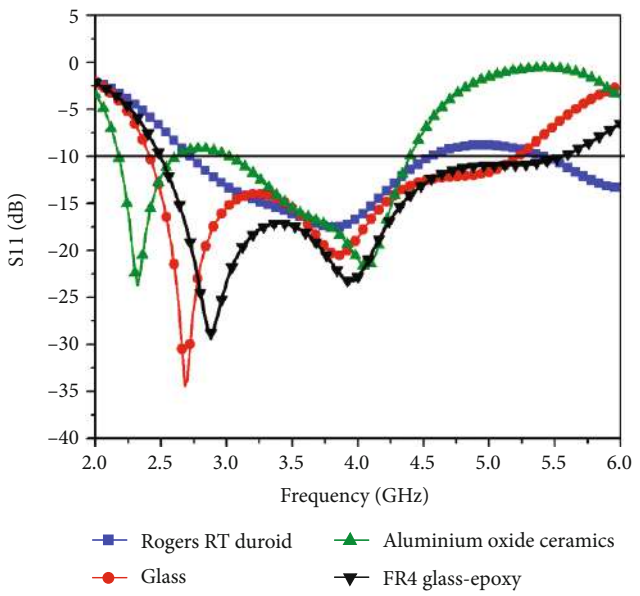

Figure 8: Comparison of S_{11} characteristics for various different substrates.

transmission line that is delivering power to the antenna and the antenna input impedance, there will be no reflection of power from the input terminals, and the supplied power will be effectively delivered to the antenna, part of which is radiated and some power is dissipated in the form of losses. The input impedance is a complex quantity with the relation as follows:

$$Z = R + jX. \tag{6}$$

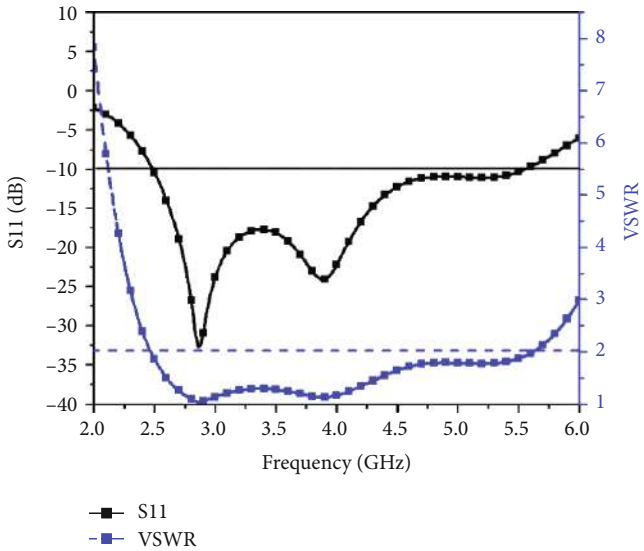

Figure 9: S_{11} and VSWR performance for the proposed antenna design.

Here, R represents the real part of impedance, termed as input resistance, with ideal value being 50 Ω in case of perfect impedance matching with the transmission line.

X represents the imaginary part of input impedance, termed as input reactance, with ideal value of zero as it represents stored power.

In Figure 4, it is seen that the proposed antenna offers 50 Ω resistance with zero reactance at 2.88 GHz, which depicts that at this frequency, perfect impedance matching for lower resonant frequency is attained by the proposed antenna.

3. Parametric Analysis for Significant Design Parameters

Certain design parameters of the proposed antenna structure play a substantial role in attaining wide impedance bandwidth between 2.5 and 5.5 GHz. These design parameters are optimized using parametric analysis in order to achieve the desired performance for the proposed antenna. The analysis is performed using the Optimetrics tool available with the electromagnetic solver HFSS (high-frequency structure simulator) version 15.0. The selected geometry variables are defined as independent variables during the design process. These independent variables are varied automatically within the constrained range using the Optimetrics tool, and the S parameter is analyzed as dependent user-defined cost function that is optimized to achieve wide impedance bandwidth. The resultant optimization tool has provided a convenient approach for automatizing the optimum value of geometry variables within short time and with less human intervention, thus providing benefit over conventional procedure of trail-and-error-based antenna designing.

S_{11} parameters, also known as return loss, signify how much input power is reflected back from the antenna. If S_{11} is less than -10 dB at a particular frequency, it depicts that more than 90% input power is accepted or radiated by the antenna for that frequency while less that 10% input

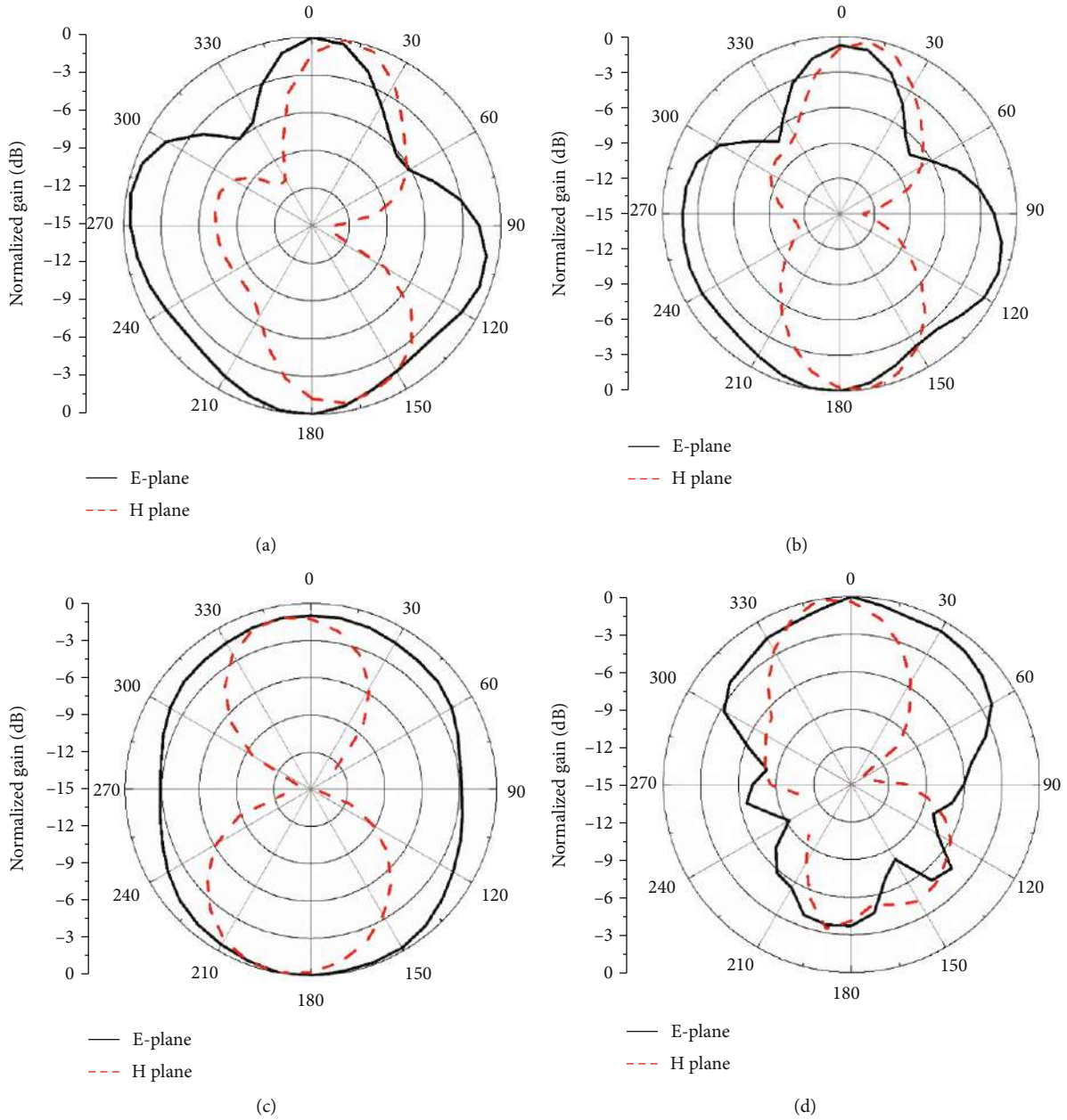

Figure 10: E-plane and H-plane radiation pattern at (a) 2.5 GHz, (b) 2.86 GHz, (c) 3.88 GHz, and (d) 5.5 GHz.

power is reflected back by the antenna which is considered return loss. It is an acceptable industry standard that the antenna responds satisfactorily at that frequency, for which return loss is less than -10 dB. Thus, S_{11} characteristics are used for parametric analysis in this section. The first design parameter that is optimized is length of the microstrip line feed, specified as L_F in Figure 5. The feed length is varied between 12 and 18 mm with uniform incremental values of 1 mm, and return loss characteristics are observed for analyzing the impedance matching over the wide frequency region. It is observed that with the feed length of 12 and 13 mm, almost the entire frequency band is above -10 dB value, thus making this length unsuitable for the proposed design. However, when the feed length is increased to 14 mm, the narrow bandwidth is obtained at 3.4 GHz resonant frequency. With the aim of wide-impedance bandwidth, the feed length is further increased to values beyond 14 mm. With the analysis of return loss characteristics, it is inferred that with the feed length of 15 mm, the minimum return loss is attained in the desired frequency band along with the widest achievable bandwidth.

The second design parameter which is analyzed is feed width, specified as W_F in Figure 6. The microstrip feed width is varied from 2.5 mm to 5 mm with increments of 0.5 mm between each variation. The graph obtained in Figure 6 clearly signifies that on increasing the width of the feed line, the return loss performance starts improving with the finest performance achieved at a width of 4 mm as the graph shows the maximum reduction in the return loss at this width at 2.86 GHz along with a wide bandwidth between

2.5 and 5.5 GHz which is our proposed band of the antenna. The graph also shows that for a width of 4.5 and 5 mm, there is no impedance matching at all proving this width to be unacceptable for the proposed design.

In addition to variation in feed width and length, the ground plane length is also varied and analyzed to attain optimum performance as shown in Figure 7. The variation is done from 4 mm to 24 mm with increments of 4 mm each. An additional simulation is also done for the conventional ground plane. The length variation performance graphs indicate that for 2.5 to 5.5 GHz band, the ground plane length of 12 mm exhibits maximum reduction in the return loss along with wide bandwidth. Although the lengths of 4 mm and 8 mm also exhibit acceptable return loss, the bandwidth is quite narrow for these cases. It is also evident that the conventional ground plane is also totally unacceptable as the return loss is above -10 dB for the entire frequency range.

There are many other alternatives available which can be considered to be used as substrate as recommended by Rani and Singh [24]. These are Rogers RT/Duroid 5880 tm (dielectric constant 2.2), glass (dielectric constant 5.5), and aluminium oxide ceramic (dielectric constant 9.8). The S_{11} parameters have been analyzed for all these substrates as shown in Figure 8.

It is clear from the above graph that when Rogers RT Duroid 5880 tm (with dielectric constant 2.2) is selected as a substrate, the return loss characteristics are below -10 dB for frequency range between 2.74 and 4.56 GHz; thus, the resulting bandwidth is 1.82 GHz. On the contrary, if glass (with dielectric constant 5.5) is used as the substrate, the 10 dB response is attained between 2.42 and 5.22 GHz, with increase in total attainable bandwidth to 2.8 GHz. With use of aluminium oxide ceramide as the substrate, bandwidth is reduced as dual band performance is achieved between 2.18–2.6 GHz and 3.02–4.38 GHz, respectively. However, when FR4-epoxy is considered as the substrate, the maximum bandwidth of 3.04 GHz is acquired between 2.5 and 5.54 GHz. Thus, with the aim of obtaining the maximum 10 dB bandwidth, the FR4-epoxy substrate is chosen as the substrate for the final antenna design.

4. Results and Discussions

Figure 9 indicates return loss characteristics along with VSWR performance for the optimized antenna design. It can be seen that the return loss S_{11} is reasonably appropriate for the optimized parameters and lies between the frequency bands for which our antenna has been proposed, i.e., 2.5-5.5 GHz. VSWR represents the voltage standing wave ratio, which is another crucial parameter for measuring how much power is reflected back by the intended antenna to the transmitter. The industry acceptable standard is to get the VSWR value less than 2 at the frequency region of interest which signifies that more than 90% input power is accepted by the antenna. The VSWR response being less than 2 is also in consonance with the proposed band as observed from Figure 9.

Figure 10(a)–10(d) represent the E-plane and H-plane radiation pattern for the frequencies 2.5 GHz, 2.86 GHz, 3.88 GHz, and 5.5 GHz, respectively. Here, 2.5 GHz is the starting frequency while 5.5 GHz is the ending frequency in the attained wideband for the anticipated antenna, while 2.86 GHz and 3.88 GHz are the lower and upper resonant frequencies in the achieved bandwidth, respectively.

It can be interpreted from the radiation pattern graphs of Figure 10 that the E-plane pattern is nearly omnidirectional for all frequencies between 2.5 and 5.5 GHz and would demonstrate to be suitable for all applications in this range. However, it is observed that at 5.5 GHz, the radiation pattern for E-plane deteriorates slightly at the bottom end due to splitting of radiation lobes. The H-plane pattern also maintains radiation uniformity and is bidirectional for all the cases except for a minor variation for 5.5 GHz.

5. Conclusion

An optimized three-petalled flower like compact wideband microstrip patch antenna is proposed in this article which is suitable for IoT-based applications. The partial ground plane is appended at the opposite end of the substrate to achieve the impedance matching over the wide frequency region between 2.5 and 5.5 GHz. The parametric analysis is conducted for feed length and feed width along with the partial ground plane in order to optimize the design using constrained and linearly convergent active optimization algorithm in the simulator so as to yield the desired results with reduced human efforts and time. The radiation symmetry is attained for various frequencies between the desired frequency bands (2.5–5.5 GHz) that demonstrate its suitability for various wireless portable applications in S-band and lower C-band frequency region. It can work in the frequency ranges of WLAN and Wi-Fi which make the antenna suitable for IoT applications, particularly operational in the unlicensed ISM band.

Data Availability

The data will be provided upon request.

Conflicts of Interest

The authors declare that they have no conflict of interest.

References

[1] A. Ghaffar, W. A. Awan, A. Zaidi, N. Hussain, S. M. Rizvi, and X. J. Li, "Compact ultra wide-band and tri-band antenna for portable device," *Radio Engineering*, vol. 29, no. 4, pp. 601–608, 2020.

[2] A. Kaur and P. K. Malik, "Multiband elliptical patch fractal and defected ground structures microstrip patch antenna for wireless applications," *Progress In Electromagnetics Research B*, vol. 91, pp. 157–173, 2021.

[3] P. Tiwari and P. K. Malik, "Design of UWB antenna for the 5G mobile communication applications: a review," in *International Conference on Computation, Automation and*

Knowledge Management (ICCAKM), pp. 24–30, Dubai, United Arab Emirates, January 2020.

[4] A. Kumar, N. Gupta, and P. C. Gautam, "Gain and bandwidth enhancement techniques in microstrip patch antennas - a review," *International Journal of Computer Applications*, vol. 148, no. 7, pp. 9–14, 2016.

[5] N. Gupta, J. Saxena, K. S. Bhatia, and R. Kumar, "A compact CPW-fed planar stacked circle patch antenna for wideband applications," *Wireless Personal Communications*, vol. 116, no. 4, pp. 3247–3260, 2021.

[6] P. K. Malik, R. Sharma, R. Singh et al., "Industrial Internet of things and its applications in industry 4.0: state of the art," *Computer Communications*, vol. 166, pp. 125–139, 2021.

[7] A. Priyanka, M. Parimala, K. Sudheer, R. Kaluri, K. Lakshmanna, and M. P. K. Reddy, "Big data based on healthcare analysis using IOT devices," in *IOP Conference Series: Materials Science and Engineering*, pp. 1–6, Institute of Physics Publishing, 2017.

[8] S. K. Vyshnavi Das and T. Shanmuganantham, "Design of multiband microstrip patch antenna for IOT applications," in *IEEE International Conference on Circuit and Systems (ICCS)*, pp. 87–92, Thiruvananthapuram, India, December 2017.

[9] J. Colaco and R. B. Lohani, "Metamaterial based multiband microstrip patch antenna for 5G wireless technology-enabled IoT devices and its applications," *Journal of Physics*, vol. 2070, pp. 1–11, 2021.

[10] A. A. Elijah and M. Mokayef, "Miniature microstrip antenna for IoT application," *Materials Today: Proceedings*, vol. 29, pp. 43–47, 2020.

[11] R. Kaluri, D. S. Rajput, Q. Xin et al., "Roughsets-based approach for predicting battery life in IoT," *Intelligent Automation and Soft Computing*, vol. 27, no. 2, pp. 453–469, 2021.

[12] G. S. Gaba, M. Hedabou, P. Kumar, A. Braeken, M. Liyanage, and M. Alazab, "Zero knowledge proofs based authenticated key agreement protocol for sustainable healthcare," *Sustainable Cities and Society*, vol. 80, p. 103766, 2022.

[13] A. Azougaghe, Z. Kartit, M. Hedabou, M. Belkasmi, and M. El Marraki, "An efficient algorithm for data security in cloud storage," in *International Conference on Intelligent Systems Design and Applications, ISDA*, pp. 421–427, Marrakech, Morocco, December 2016.

[14] M. Hedabou and Y. S. Abdulsalam, "Efficient and secure implementation of BLS multisignature scheme on TPM," in *Proceedings -2020 IEEE International Conference on Intelligence and Security Informatics, ISI*, pp. 1–6, Arlington, VA, USA, November 2020.

[15] Y. S. Abdulsalam and M. Hedabou, "Security and privacy in cloud computing: technical review," *Future Internet*, vol. 14, no. 1, p. 11, 2022.

[16] Y. Etiabi, E. M. Amhoud, and E. Sabir, "A distributed and collaborative localization algorithm for Internet of things environments," in *Proceedings of the 18th International Conference on Advances in Mobile Computing & Multimedia*, pp. 114–118, Chiang Mai Thailand, 2020.

[17] S. Lhazmir, O. A. Oualhaj, A. Kobbane, E. M. Amhoud, and J. Ben-Othman, "UAV for wireless power transfer in IoT networks: a GMDP approach," in *IEEE International Conference on Communications*, pp. 1–6, Dublin, Ireland, June 2020.

[18] M. Jouhari, E. M. Amhoud, N. Saeed, and M. S. Alouini, "A survey on scalable LoRaWAN for massive IoT: recent advances, potentials, and challenges," *Networking and Internet Architecture, Cornell University*, 2022, http://arxiv.org/abs/2202.11082.

[19] N. Gupta, J. Saxena, and K. S. Bhatia, "Design of wideband flower-shaped microstrip patch antenna for portable applications," *Wireless Personal Communications*, vol. 109, no. 1, pp. 17–30, 2019.

[20] H. T. Chattha, M. Hanif, X. Yang, I. E. Rana, and Q. H. Abbasi, "Frequency reconfigurable patch antenna for 4G LTE applications," *Progress in Electromagnetics Research*, vol. 69, pp. 1–13, 2018.

[21] D. Tripathi, D. K. S. Ramesh, and K. Verma, "Bandwidth enhancement of slotted rectangular wideband microstrip antenna for the application of WLAN/WiMAX," *Wireless Personal Communications*, vol. 119, no. 2, pp. 1193–1207, 2021.

[22] M. A. Khan, M. A. Ul Haq, and R. S. Ur, "A practical miniature antenna design for future Internet of things enabled smart devices," in *10th International Conference on Signal Processing and Communication Systems, ICSPCS*, Surfers Paradise, QLD, Australia, December 2016.

[23] T. Varum, A. Ramos, J. Caiado, and J. N. Matos, "Wideband series-fed microstrip antenna array for 5G/IoT systems," in *12th International Symposium on Communication Systems, Networks and Digital Signal Processing, CSNDSP*, pp. 1–4, Porto, Portugal, July 2020.

[24] S. Rani and A. P. Singh, "A novel design of hybrid fractal antenna using BFO," *Journal of Intelligent and Fuzzy Systems*, vol. 27, no. 3, pp. 1233–1241, 2014.

[25] W. M. Abdulkawi, A. F. A. Sheta, I. Elshafiey, and M. A. Alkanhal, "Design of low-profile single-and dual-band antennas for IoT applications," *Electronics (Basel)*, vol. 10, no. 22, p. 2766, 2021.

[26] R. Ramasamy, V. Rajavel, and V. Babu, "Design and analysis of multiband bloom shaped patch antenna for IoT applications," *Turkish Journal of Computer and Mathematics Education (TURCOMAT)*, vol. 12, pp. 4578–4585, 2021.

[27] M. S. Islam, M. T. Islam, M. A. Ullah, G. K. Beng, N. Amin, and N. Misran, "A modified meander line microstrip patch antenna with enhanced bandwidth for 2.4 GHz ISM-band Internet of things (IoT) applications," *IEEE Access*, vol. 7, pp. 127850–127861, 2019.

[28] G. T. Reddy, M. P. K. Reddy, K. Lakshmanna et al., "Analysis of dimensionality reduction techniques on big data," *IEEE Access*, vol. 8, pp. 54776–54788, 2020.

[29] K. Lakshmanna and N. Khare, "Constraint-based measures for DNA sequence mining using group search optimization algorithm," *International Journal of Intelligent Engineering and Systems*, vol. 9, no. 3, pp. 91–100, 2016.

[30] R. Chandel, A. K. Gautam, and K. Rambabu, "Tapered fed compact UWB MIMO-diversity antenna with dual band-notched characteristics," *IEEE Transactions on Antennas and Propagation*, vol. 66, no. 4, pp. 1677–1684, 2018.

[31] K. G. Thomas and M. Sreenivasan, "A simple ultrawideband planar rectangular printed antenna with band dispensation," *IEEE Transactions on Antennas and Propagation*, vol. 58, no. 1, pp. 27–34, 2010.